Available online at www.sciencedirect.com

SciVerse ScienceDirect

Physics Procedia 39 (2012) 569 – 576

Physics Procedia

LANE 2012

Pulsed Nd:YAG laser welding of Ni-alloy Hastelloy C-276 foils

Vicente Afonso Ventrella[a,*], José Roberto Berretta[b], Wagner de Rossi[b]

[a]*Universidade Estadual Paulista-UNESP, Departamento de Engenharia Mecânica, 15.385-000, Ilha Solteira, Brazil*
[b]*Instituto de Pesquisas Energéticas e Nucleares-IPEN, Centro de Lasers e Aplicações, 05.508-900, São Paulo, Brazil*

Abstract

In this study a pulsed Nd:YAG laser was used to join Hastelloy C-276 thin foil with 100 microns thickness. Pulse energy was varied from 1.0 to 2.25 J at small increments of 0.25 J with a 4 ms pulse duration. The macro and microstructures of the welds were analyzed by optical and electronic microscopy, tensile shear test and microhardness. Sound laser welds without discontinuities were obtained with 1.5 J pulse energy. Results indicate that using a precise control of the pulse energy, and so a control of the dilution rate, it is possible to weld Hastelloy C-276 thin foil by pulsed Nd:YAG laser.

Keywords: Laser welding; Nd:YAG; Hastelloy C-276; Thin foil; Tensile shear test

1. Introduction

Nickel-based alloys constitute an important class of materials, which are used under demanding conditions of high corrosion resistance and high temperature strength. These characteristics together with their good ductility and easy of cold working make them generally very attractive for a wide variety of applications; nearly all of which exploit their corrosion resistance in atmospheric, salt water and various acid and alkaline media. Ni-Cr-Mo-W alloys, named as Hastelloy, are used for marine engineering, chemical and hydrocarbon processing equipment, valves, pumps, sensors and heat exchangers. Hastelloy C-276 has been successfully applied in the chemical engineering field due to its satisfactory corrosion resistance to HCl [1, 2]. Welding thin foil materials is very important in many industrial applications. The need for joints between thin foils often appears in complex components, especially the combination with

* Corresponding author. Tel.: +55-18-3743-1095 ; fax: +55-18-3742-2992 .
E-mail address: ventrella@dem.feis.unesp.br .

1875-3892 © 2012 Published by Elsevier B.V. Selection and/or review under responsibility of Bayerisches Laserzentrum GmbH
doi:10.1016/j.phpro.2012.10.075

a more corrosion resistant material. Due to differences in thermal conductivity, fusion temperature and solubility of the materials, brittle phases can appear and deteriorate the tensile strength of the joint. Pulsed laser systems have the capability to weld different materials without filler metal (autogenous welding), with high energy density and low heat-input [3].

Welding with pulsed Nd:YAG Laser System is characterized by periodic heating of the weld pool by a high peak power density pulsed laser beam incident that allow melting and solidification to take place consecutively. However, due to very high peak power density involved, the solidification time is shorter than continuous laser and conventional welds. Combination of process parameters such as pulse energy [Ep], pulse duration [tp], repetition rate [Rr], beam spot size [Φb] and welding speed [v] determines the welding mode, that is, conduction or keyhole [4, 5].

Research examining the Nd:YAG laser for continuous welding, pulsed welding, dissimilar sheet welding and coated sheet welding has been published. Kim et al.[6] reported successful welding of Inconel 600 tubular components of nuclear power plant using a pulsed Nd:YAG laser. Ventrella et al.[7] using a millisecond Nd:YAG Pulsed Laser System studied lap joint welding of austenitic AISI 316L thin foils. Ping and Molian [8] utilized a nanosecond pulsed Nd:YAG laser system to weld 60 μm of thin AISI 304 stainless steel foil.

The present work has been carried out to investigate the influence of the pulse energy on neodymium: yttrium aluminum garnet (Nd:YAG) laser welding of Hastelloy C-276 thin foil and its effect on weld joint characteristics.

2. Experimental

This study used a millisecond pulsed Nd:YAG laser system, and its experimental setup is shown in Fig. 1.

Hastelloy C-276 with thickness of 100 μm was used as base metal; its detailed chemical composition is shown in Table 1. Before welding, the specimens were cleaned and held firmly using a jig to fix and prevent absence of contact and excessive distortion of the thin foil.

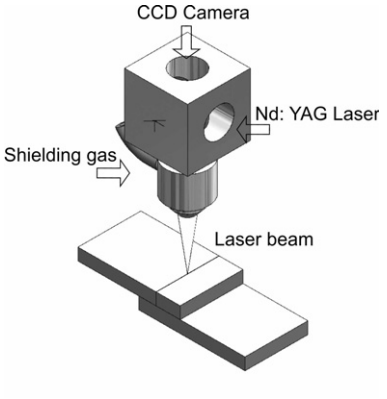

Fig. 1. Experimental setup of the laser system

Tab. 1. Chemical compositions (*wt %*) of Hastelloy C-276

Element	C	Ni	Cr	Mo	Mn	Fe	Co	W
wt. %	0.01	Bal.	15.9	15.6	0.52	5.35	1.51	3.38

To evaluate the influence of the pulse energy, welding was performed using specimens positioned as lap joints. They were welded with a beam spot size (Φb) and beam angle (Ab) of 0.2 mm and 90 degrees, respectively. The focus point was fixed on the surface of the work-piece. The welding speed (v) and repetition rate (Rr) were fixed at 500 mm/min and 39 Hz, respectively. The pulse energy (Ep) varied from 1.0 to 2.25 J at increments of 0.25 J with a 4 ms pulse duration (tp). Thus, there was one controlled parameter in this process: the pulse energy. The specimens were held firmly using a jig, to fix and prevent absence of contact and excessive distortion. Fixing is extremely important for thin-section laser welding. Tolerances were held closely to maintain joint fitups without allowing either mismatch or gaps.

The specimens were laser-welded in an argon atmosphere at a flow rate (Fr) of 10 l/min. Back shielding of the joint was not necessary because Hastelloy C-276 is not an oxidizable metal like Al and Ti. None of the specimens were subjected to any subsequent form of heat treatment or machining. After welding, the specimens were cut for the tensile-shear tests, as shown in Fig. 2. Finally, part of the cut surfaces was prepared for metallographic inspection by polishing and etching to display a bead shape and microstructure. Metallographic samples were prepared with a solution of nitric and hydrochloric acid. The bead shape measurements were made using an optical microscope with an image analysis system. Fig. 3 shows a schematic illustration of the transverse joint section with the analyzed geometric parameters.

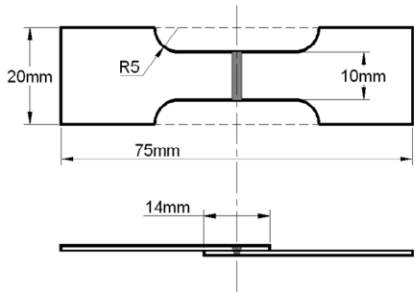

Fig. 2. Schematic diagram of tensile test specimen design

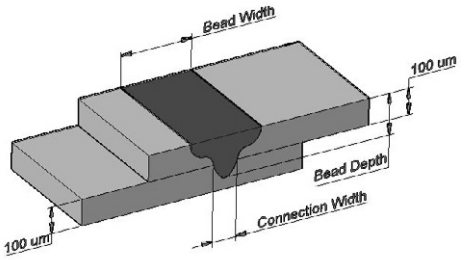

Fig. 3. Lap joint configuration with the analyzed geometric parameters

The strength of the welds was evaluated using Vickers microhardness and tensile shear strength tests. Microhardness tests were performed on a transverse section of the weld bead, parallel to the surface of the thin foils, in the region next to the connection line of the top foil. Microhardness tests identify possible effects of microstructural heterogeneities in the fusion zone and in the base metal. The reported data were the average of five individual results. For the tensile shear test, specimens were extracted from welded samples, and the width of the samples was reduced to 10 mm to lower the load required to fracture them.

3. Results and Discussion

The weld beads showed characteristic of pulsed laser welding. No welding cracks were found in any of the welds; this may be partly due to the good crack resistance of base the metals and the correct welding parameters. No discontinuities were observed in the fusion metal of the beads, which demonstrates the efficiency of the shielding gas in preventing oxidation, large porosities and gas inclusions, which cause poor weld quality. All specimens were welded in the conduction mode.

Fig. 4a shows a specimen welded with 2.25 J pulse energy for the tensile shear test and Fig. 4b shows a top view of the weld bead. It is clearly noticeable in Fig. 4b no detectable defect existed on the surface of the weld bead or adjacencies.

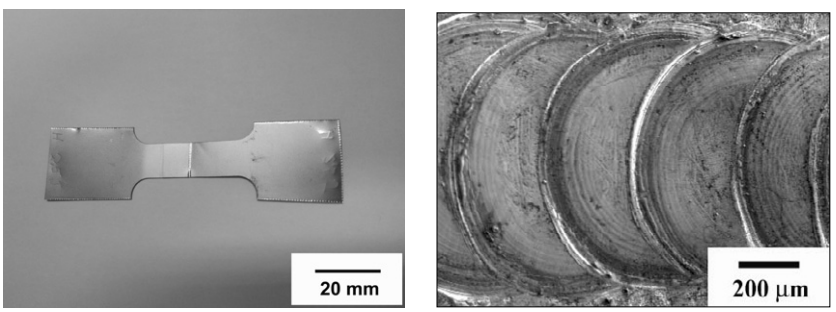

(a) (b)

Fig. 4. (a) Welded specimen for the tensile shear test; (b) and a pulsed weld bead

The macroscopic examination of the cross sections of all specimens also indicated that the weld pool morphology is essentially symmetrical about the axis of the laser beam. This symmetry at the top and

bottom was observed in all joints independent of the pulse energy, which suggests a steady fluid flow in the weld pool; however, as the pulse energy increased, a high depression was formed at the top.

The cross section macrostructures of lap laser welds as a function of pulse energy (Ep) are summarized in Fig. 5. In Figs. 5a and 5b (specimens with 1.0 and 1.25 J pulse energy, respectively) no penetration at the bottom sheet and no depression at the top of the bead was observed, probably due to insufficient energy to bridge the couple. It is clearly noticeable in Figs. 5a and 5b the presence of a small gap between couple. The macrostructures showed that melting started at the surface irradiated by the laser beam and the molten pool grew continuously to axial and radial axis. Due to the thin thickness, low pulse energy of the laser beam and the presence of a small gap, the molten pool just grew in the radial direction of the top foil resulting in a no bonded joint with the weld morphology observed in Figs. 5a and 5b. Gaps between foils and gaps in the connection line increase stress and thus are detrimental to weld quality in terms of mechanical properties. As reported in the literature [9] the presence of wider gaps in welded joints result in more deeply concave underfills. Specimens welded in the present work with low pulse energy, 1.0 and 1.25 J, present no underfill because the molten material did not have enough time to fill the gap. When the pulse energy was increased on the other specimens, a connection region between the foils was observed, as shown in Fig. 5c (welded with 1.5 J). Both specimens present no underfill and no excess of molten material at the root. The penetration depth increased as the pulse energy increased. Both joints present an intimate contact between the couples (absence of gap). These specimens present excellent conditions for laser seam welding. In Figs. 5e and 5f (specimens with 2.0 and 2.25 J pulse energy, respectively), an increase occurred with a depression at the top and a penetration bead. The concavity increased proportionally to the pulse energy (Ep). Moreover, it was evident that specimens welded with 2.0 and 2.25 J pulse energy undergo deformation during joint welding, which causes a large bending moment. Areas near the heat source of the upper foil are heated to higher temperatures and thus expand more than areas away from the heat source or regions of the lower foil. After the foil cools to the initial temperature, the final deformation remains. Like the material heated by the laser beam, the irradiance did not cause the material reach its boiling point; no significant amount of surface material was removed.

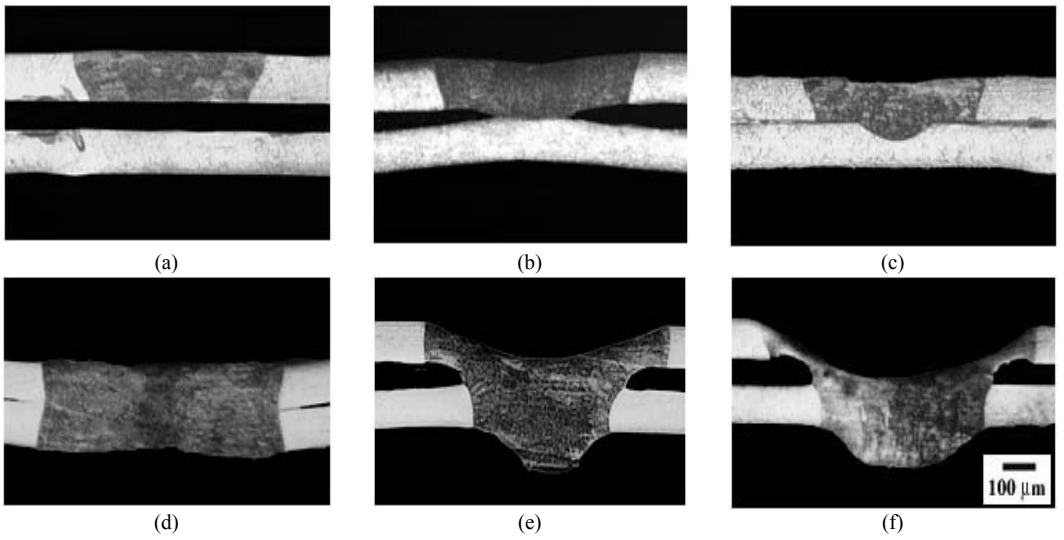

Fig. 5. Cross sections of Hastelloy C-276 lap joints made with pulsed Nd:YAG laser welding with different pulse energies (Ep): (a) 1.0 J; (b) 1.25 J; (c) 1.50 J; (d) 1.75 J; (e) 2.0 J; (f) 2.25 J; All figures have the same magnification as shown in (f)

The relationship between pulse energy and weld metal geometry of Hastelloy C-276 is summarized in Fig. 6. The bead width increased from 576 to 772 μm as pulse energy varied from 1.0 to 2.0 J. This indicated that when the laser beam interacts with the specimen, it creates a liquid melt pool by absorbing the incident radiation. This bead width variation is a result of the higher pulse energy; a high amount of material is molten and then propagates through the base material. In the presence of high pulse energy, part of the melt material passed through the joint, which increased the concavity at the top of the weld, the excess of weld metal at the root and the heat-affected zone extension. On the other hand, at a pulse energy of 2.25 J, the molten metal volume decreased, and deep concave underfills occurred.

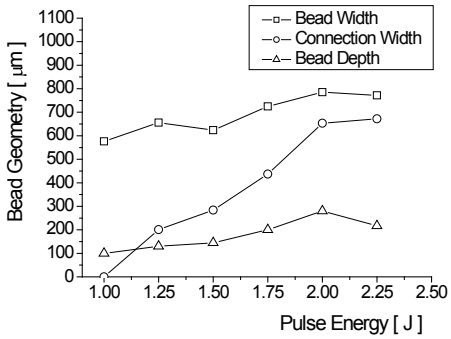

Fig. 6. Bead geometry as a function of pulse energy [Ep]

The ultimate tensile strength (UTS) tends to increase at first and then decrease as the pulse energy (Ep) increases. The relationship between pulse energy and tensile shear strength of welded joints is summarized in Fig. 7. Specimens welded with pulse energy lower than 1.25 J were not bonded because the pulse energy was too low, and the molten pool did not have enough time to propagate to the bottom foil; incomplete penetration occurred. Otherwise, when the specimens were welded with pulse energy greater than 1.75 J, excessive underfilling and burnthrough was observed. Perforations in the weld bead were observed with pulse energy higher than 2.25 J.

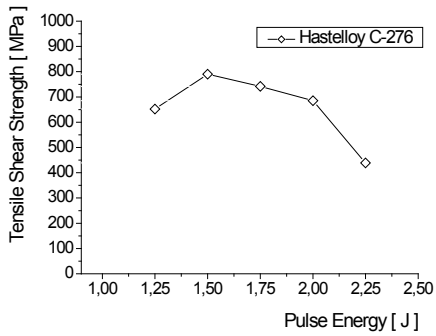

Fig. 7. Relationship between pulse energy and tensile shear strength

The failure of all specimens occurs in the region next to the fusion line of the top foil. This is expected because hardness and tensile strength values are known to be related. Moreover, the thickness of the top foil is reduced as pulse energy increases. Fig. 8 shows a top view of the region fractured resulting from the tensile shear tests of the sample Hastelloy C-276. All samples ruptured in the fusion line. It was observed, in all of them, a thickness reduction of the sheet.

The tensile properties of the welded joint affected by pulse energy (Ep) can be explained by macro and microstructural analyses. As the pulse energy increases, the grains in the weld metal and in the HAZ become coarser. The heat-affected zone extension increases too. Discontinuities become more severe. Some precipitates can be present intergranularly and even continuously along the grain boundary. These microstructural changes contribute to a weakness of the weld joint, which reduces the tensile properties [10].

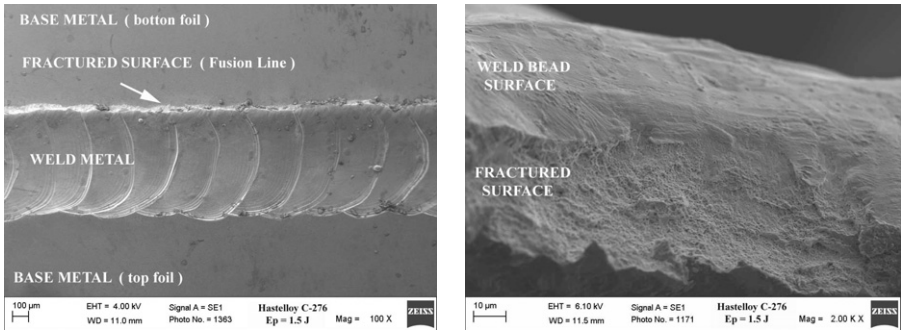

(a) (b)

Fig. 8. Top view of the joint region fractured (a) and surface fractured; (b) from the tensile shear tests. Hastelloy C-276. 1,5 J

The microhardness values decreased as the joint energy increased (1.0 J to 2.25 J) to maximum energy (2.25 J). During the solidification of the fusion zone, the material generally loses original strength that is induced by strain hardening. Microhardness profiles in welded joints obtained with lower energy show increasing of the hardness in the fusion zone and a finer microstructure that is induced by rapid cooling.

In summary, the most acceptable weld bead was obtained at pulse energy of 1.5 J, where the molten pool bridged the couple and the weld bead profile showed minimum underfill. The tensile shear test exhibited 790 MPa. No undercut and minimum porosity were observed. No evidence of hot cracking was observed in the weld metal and this is attributed to the rapid solidification conditions typical of the pulsed Nd:YAG laser welding process.

4. Conclusions

The results obtained from this study demonstrate that is possible to weld 100 µm thickness Hastelloy C-276 thin foils, in terms of microstructural and mechanical reliability, by precisely controlling the laser pulse energy. The better performance was due to the high quality joint; a joint marked by good penetration, no underfill and free from microcracks and porosity. This was obtained at an energy pulse of 1.5 J, a repetition rate [Rr] of 39 Hz and a 4 ms pulse duration. This reflects one of the most notable features of pulsed laser welding compared with other processes; welding with low heat input. The work also shows that the process is very sensitive to the gap between couples which prevents good heat transfer between the foils. The shape and dimensions of the thin foil weld bead observed in the present work

depended not only on the pulse energy, but also on the presence of gaps between foils. Bead width, connection width and bead depth increased as the pulse energy increased. The ultimate tensile strength (UTS) of the welded joints initially increased and then decreased as the pulse energy increased. The specimen welded with 1.5 J attained the maximum tensile shear strength. In all the specimens, fracture occurred in the top foil fusion line. The microhardness was almost uniform across the parent metal, HAZ and weld metal. A slight increase in the fusion zone compared to those measured in the base metal was observed. This is related to the microstructural refinement in the fusion zone, induced by rapid cooling.

Acknowledgements

The authors gratefully acknowledge the financial support of CNPq.

References

[1] Zhang, Q.; Tang, R.; Yin, K.; Luo, X.; Zhang, L.: Corrosion behavior of Hastelloy C-276 in supercritical water. *CSci.* 2009; 51: pp. 2092–2097.

[2] Singh,V.B.; Gupta, A.: The electrochemical corrosion and passivation behavior of Monel 400 in concentrated acids and their mixtures. *Transaction of JWRI.* 2000; 34: pp. 19–23.

[3] Gilner,A.; Holtkamp, J.; Hartmann, C.; Olowinsky, A.; Gedicke, J.; Klages, K.; Bosse, K.: Laser applications in microtechnology. *JMPT*. 2005; 167: pp. 494-498.

[4] Duley, W. W.: *Laser Welding*. 3rd ed. New York: John Wiley & Sons; 1999.

[5] Steen, W. M.: *Laser Material Processing*. 3rd ed. London: Springer; 2005.

[6] Kim, D.J.; Kim, C.J.; Chung, C.M.: Repair welding of etched tubular components of nuclear power plant by Nd:YAG laser. *JMPT*. 2001, 14: pp. 51-56.

[7] Ventrella, V.A.; Berretta, J.R.; Rossi, W.: Pulsed Nd:YAG laser seam welding of AISI 316L stainless steel thin foils. *JMPT*. 2010, 210: pp. 1838-1843.

[8] Ping, D.; Molian, P.: Q-switch Nd:YAG laser welding of AISI stainless steel foils. *MSci&Eng. A*. 2008, 486: pp. 680-685.

[9] Kawarito, Y.; Kito, M.; Katayama, S.: In-process monitoring and adptive control for gap in microbutt welding with pulsed YAG laser. *JPh D*: *APh*, 2007. 40: pp. 183-190.

[10] Quan,Y.J.; Chen,Z.H.; Gong,X.S.; Yu,Z.H.: Effects of heat input on microstructures and tensile properties of laser welded magnesium alloy. *MChar*, 2008. 59: pp. 1491-1497.